



University of Southern Denmark

## The thick left ventricular wall of the giraffe heart normalises wall tension, but limits stroke volume and cardiac output

Smerup, Morten; Damkjær, Mads; Brøndum, Emil; Baandrup, Ulrik T; Kristiansen, Steen Buus; Nygaard, Hans; Aalkjær, Christian; Sauer, Cathrine; Buchanan, Rasmus; Bertelsen, Mads Frost; Østergaard, Kristine; Grøndahl, Carsten; Candy, Geoffrey; Hasenkam, J Michael; Secher, Niels H; Bie, Peter; Wang, Tobias

*Published in:*

The Journal of Experimental Biology

*DOI:*

10.1242/jeb.132753

*Publication date:*

2016

*Document version:*

Final published version

*Citation for pulished version (APA):*

Smerup, M., Damkjær, M., Brøndum, E., Baandrup, U. T., Kristiansen, S. B., Nygaard, H., Aalkjær, C., Sauer, C., Buchanan, R., Bertelsen, M. F., Østergaard, K., Grøndahl, C., Candy, G., Hasenkam, J. M., Secher, N. H., Bie, P., & Wang, T. (2016). The thick left ventricular wall of the giraffe heart normalises wall tension, but limits stroke volume and cardiac output. *The Journal of Experimental Biology*, 219, 457-463.

<https://doi.org/10.1242/jeb.132753>

Go to publication entry in University of Southern Denmark's Research Portal

### Terms of use

This work is brought to you by the University of Southern Denmark.

Unless otherwise specified it has been shared according to the terms for self-archiving.

If no other license is stated, these terms apply:

- You may download this work for personal use only.
- You may not further distribute the material or use it for any profit-making activity or commercial gain
- You may freely distribute the URL identifying this open access version

If you believe that this document breaches copyright please contact us providing details and we will investigate your claim. Please direct all enquiries to [puresupport@bib.sdu.dk](mailto:puresupport@bib.sdu.dk)

## RESEARCH ARTICLE

# The thick left ventricular wall of the giraffe heart normalises wall tension, but limits stroke volume and cardiac output

Morten Smerup<sup>1,2</sup>, Mads Damkjær<sup>3,4,\*</sup>, Emil Brøndum<sup>5,6</sup>, Ulrik T. Baandrup<sup>7</sup>, Steen Buus Kristiansen<sup>8</sup>, Hans Nygaard<sup>9</sup>, Jonas Funder<sup>9</sup>, Christian Aalkjær<sup>5,6</sup>, Cathrine Sauer<sup>10</sup>, Rasmus Buchanan<sup>11</sup>, Mads Frost Bertelsen<sup>10</sup>, Kristine Østergaard<sup>7</sup>, Carsten Grøndahl<sup>10</sup>, Geoffrey Candy<sup>12</sup>, J. Michael Hasenkam<sup>9</sup>, Niels H. Secher<sup>13</sup>, Peter Bie<sup>4</sup> and Tobias Wang<sup>11</sup>

## ABSTRACT

Giraffes – the tallest extant animals on Earth – are renowned for their high central arterial blood pressure, which is necessary to secure brain perfusion. Arterial pressure may exceed 300 mmHg and has historically been attributed to an exceptionally large heart. Recently, this has been refuted by several studies demonstrating that the mass of giraffe heart is similar to that of other mammals when expressed relative to body mass. It thus remains unexplained how the normal-sized giraffe heart generates such massive arterial pressures. We hypothesized that giraffe hearts have a small intraventricular cavity and a relatively thick ventricular wall, allowing for generation of high arterial pressures at normal left ventricular wall tension. In nine anaesthetized giraffes (495±38 kg), we determined *in vivo* ventricular dimensions using echocardiography along with intraventricular and aortic pressures to calculate left ventricular wall stress. Cardiac output was also determined by inert gas rebreathing to provide an additional and independent estimate of stroke volume. Echocardiography and inert gas-rebreathing yielded similar cardiac outputs of 16.1±2.5 and 16.4±1.4 l min<sup>-1</sup>, respectively. End-diastolic and end-systolic volumes were 521±61 ml and 228±42 ml, respectively, yielding an ejection fraction of 56±4% and a stroke volume of 0.59 ml kg<sup>-1</sup>. Left ventricular circumferential wall stress was 7.83±1.76 kPa. We conclude that, relative to body mass, a small left ventricular cavity and a low stroke volume characterizes the giraffe heart. The adaptations result in typical mammalian left ventricular wall tensions, but produce a lowered cardiac output.

**KEY WORDS:** Echocardiography, Left ventricle, End diastolic volume, Cardiac output, Stroke volume

<sup>1</sup>Department of Cardiothoracic Surgery, Rigshospitalet, 2100 Copenhagen, Denmark. <sup>2</sup>Department of Clinical Medicine, Aarhus University, 8000 Aarhus, Denmark. <sup>3</sup>Hans Christian Andersen Children's Hospital, 5000 Odense, Denmark. <sup>4</sup>Department of Cardiovascular and Renal Research, University of Southern Denmark, 5000 Odense, Denmark. <sup>5</sup>Department of Biomedicine, Aarhus University, 8000 Aarhus, Denmark. <sup>6</sup>Department of Biomedical Sciences, Copenhagen University, 2200 Copenhagen, Denmark. <sup>7</sup>Department of Pathology, Center for Clinical Research, Vendsyssel Hospital, Aalborg University, 9000 Aalborg, Denmark. <sup>8</sup>Department of Cardiology, Aarhus University Hospital, 8200 Aarhus N, Denmark. <sup>9</sup>Department of Thoracic and Cardiovascular Surgery and Department of Clinical Medicine, Aarhus University, 8200 Aarhus N, Denmark. <sup>10</sup>Centre for Zoo and Wild Animal Health, Copenhagen Zoo, 1870 Frederiksberg C, Denmark. <sup>11</sup>Zoophysiology, Department of Biological Sciences, Aarhus University, 8000 Aarhus C, Denmark. <sup>12</sup>Department of Physiology and Medicine, University of the Witwatersrand, Parktown, 2193 Johannesburg, South Africa. <sup>13</sup>Department of Anesthesiology, Rigshospitalet, 2100 Copenhagen, Denmark.

\*Author for correspondence (mdamkjaer@health.sdu.dk)

Received 5 October 2015; Accepted 6 November 2015

## INTRODUCTION

Giraffes are the tallest extant animals on Earth and are renowned for their high mean arterial blood pressure ( $P_a$ ) at heart level (>300 mmHg in systole), which provides for typical mammalian cerebral perfusion pressures even when the brain is positioned several metres above the heart (Goetz and Budtz-Olsen, 1955; Van Citters et al., 1966, 1968, 1969; Mitchell et al., 2006; Brøndum et al., 2009). In a series of legendary studies on the influences of posture and gravity on the cardiovascular systems of giraffes, Goetz and colleagues reported that the high mean  $P_a$  is achieved by virtue of an exceptionally large heart (Goetz, 1955; Goetz and Keen, 1957). This intuitively appealing notion became widely accepted and even inspired the development of the so-called 'giraffe language' as a euphemism for compassionate communication (Rosenberg, 1999). However, several recent and independent investigations, based on much larger sample sizes than the original studies by Goetz, now reveal that giraffes are merely endowed with the same relative cardiac mass as all other mammals, i.e. 0.5–0.6% of body mass ( $M_b$ ; Brøndum et al., 2009; Mitchell and Skinner, 2009; Østergaard et al., 2013; Perez et al., 2008). Incidentally, Edwards Crisp (1864a,b) had already reported normal mammalian heart size in giraffes by the middle of the nineteenth century and Goetz's original report therefore appears erroneous (Mitchell and Skinner, 2009).

Although the normal size of the giraffe heart now appears well established, it remains enigmatic how the high mean  $P_a$  is generated. As noted by Seymour and Blaylock (2000), ventricular wall stress seems to be very similar in mammals. When the left ventricle is simplified to assume the shape of a thick-walled cylinder, the principle of Laplace states that the mechanical stress exerted on the myocardial wall is proportional to left ventricular pressure ( $P_{LV}$ ) and its midwall radius ( $r$ ), whereas it is inversely proportional to wall thickness ( $T_{wall}$ ):

$$\text{Wall stress} = \frac{P_{LV} \times r}{T_{wall}}. \quad (1)$$

Thus, an attractive possibility is that the giraffe heart has normalized wall stress in response to the high intraventricular blood pressure by having a lower left ventricular radius and a thicker ventricular wall (Mitchell and Skinner, 2009). This can be achieved by a typical mammalian heart mass relative to  $M_b$ , but must entail a lower stroke volume ( $V_S$ ) per unit of cardiac mass than in similar-sized mammals (see Fig. 1, which also shows the gross morphology of the giraffe heart). Consequently, if the heart rate of giraffes is similar to that of similar-sized mammals, then cardiac output per mass unit must be substantially lower. To investigate the hypothesis that giraffes have a volumetrically small heart with a low intraventricular radius, we

**List of symbols and abbreviations**

CWS	systolic circumferential wall stress
$D$	systolic endocardial short-axis diameter
$L$	systolic endocardial long-axis diameter
$M_b$	body mass
$P_a$	arterial pressure
$P_{a_{sys}}$	systolic arterial pressure
$P_{LV}$	left ventricular pressure
$P_{RA}$	right atrial pressure
$P_{RV}$	right ventricular pressure
$Q$	cardiac output
$r$	midwall radius of the left ventricle
SVR	systemic vascular resistance
$T_{wall}$	systolic wall thickness of the left ventricle
$V_{ED}$	end diastolic volume
$V_{ES}$	end systolic volume
$V_S$	stroke volume
$W$	work of the heart

determined left ventricular systolic and diastolic dimensions, including wall thicknesses in young anaesthetised giraffes by echocardiography. We obtained simultaneous intraventricular blood pressures to calculate ventricular wall stresses. We also performed additional and independent measurements of cardiac output using the inert gas rebreathing technique allowing us to assess  $V_S$  by two independent and principally different methods.

**MATERIALS AND METHODS**

These studies were part of the second expedition by The Danish Cardiovascular Giraffe Research Programme (DaGIR) in October–November 2010 to Hammanskraal, Gauteng Province, South Africa.

**Experimental animals**

Experiments were performed on eight juvenile male giraffes (*Giraffa camelopardalis* Linnaeus 1758) with an estimated age of 14 to 52 months, an  $M_b$  ranging from 330 to 654 kg ( $495 \pm 38$  kg; mean  $\pm$  s.e.m.) and a standing height of 3.4–3.9 m. All animals were bred for trophy hunting in Namibia and were maintained in a quarantine facility in Hammanskraal for up to 2 months prior to the experiments. The experimental protocol was approved by the national Danish Animal Experiments Inspectorate (Danish Ministry of Justice), the Animal Ethics Screening Committee at the University of Witwatersrand (Johannesburg) and the Animal Use and Care Committee (University of Pretoria). Local ethical committee members oversaw the experiments and permission to euthanise the animals was granted by the Gauteng Province of South Africa.

**Animal handling and anaesthesia**

All studies were performed on anaesthetised giraffes using an experimental protocol and a set-up as described previously by

Brøndum et al. (2009); following overnight fast and 2 h without water, the giraffes were sedated with medetomidine ( $6 \mu\text{g kg}^{-1}$ , i.m.) and guided to a chute where they were blindfolded. Anaesthesia was induced by remote injection of etorphine ( $9 \mu\text{g kg}^{-1}$ , i.m.) and ketamine ( $0.9 \text{ mg kg}^{-1}$ , i.m.), which rendered the giraffes recumbent within minutes. As soon as the animals were recumbent, a cuffed endotracheal tube (internal diameter, 20 mm) was inserted to allow ancillary ventilation with oxygen using a demand valve (Hudson RCI). After a supplementary dose of ketamine ( $0.2 \text{ mg kg}^{-1}$ , i.v.), the giraffes were placed in right lateral recumbency on a custom-made movable platform. Animals were allowed to breathe spontaneously, but were mechanically ventilated if necessary to maintain normal end-tidal  $\text{CO}_2$  and arterial blood gases. Anaesthesia was maintained by continuous infusion of  $\alpha$ -chloralose (KVL Pharmacy, Frederiksberg, Denmark;  $30 \text{ mg kg}^{-1} \text{ h}^{-1}$  gradually decreasing guided by clinical signs) into the saphenous vein. Following systemic administration of heparin ( $150 \text{ units kg}^{-1}$ ;  $25,000 \text{ IE ml}^{-1}$ ; B. Braun, Melsungen, Germany) and local infiltration by lidocaine (2%; SAD, Copenhagen, Denmark), vascular sheaths were placed in the carotid artery and jugular vein at the base of the neck. Using limb straps to avoid pressure on the thoracic and abdominal regions, the platform was used to hoist the giraffe to an upright position. To minimise the influence of the induction agents on the cardiovascular system, the effect of the etorphine was reversed with naltrexone and measurements were obtained after the effects of medetomidine and ketamine were expected to have subsided (more than 90 min after administration; Brøndum et al., 2009).

The cardiovascular measurements completed in the present study would be virtually impossible to achieve in conscious animals where the necessary restraint and handling stress would be ethically unacceptable and cause considerable disturbance to haemodynamic variables. The anaesthetics themselves also influence the cardiovascular system; however, as mentioned above, the effects of etorphine and medetomidine are considered to be very small and  $\alpha$ -chloralose is regarded to have smaller effects on circulation than most other anaesthetics and allowed for a dynamic regulation of anaesthesia depth (Covert et al., 1992).

**Measurements of cardiac output**

Cardiac output ( $Q$ ) was determined in nine spontaneously breathing giraffes using the inert gas rebreathing technique (Innocor Inert Gas Rebreather, Innovision, Glamsbjerg, Denmark; Clemensen et al., 1994). Rebreathing was performed over a minimum of five breaths to ensure complete mixing of the gases with the air in the respiratory system. The experimental site was located at approximately 1200 m above sea level, and therefore we corrected for the actual barometric pressure. The rebreathing technique provides a reliable measure of effective pulmonary blood flow (Gabielsen et al., 2002), but could underestimate systemic cardiac output in the presence of pulmonary

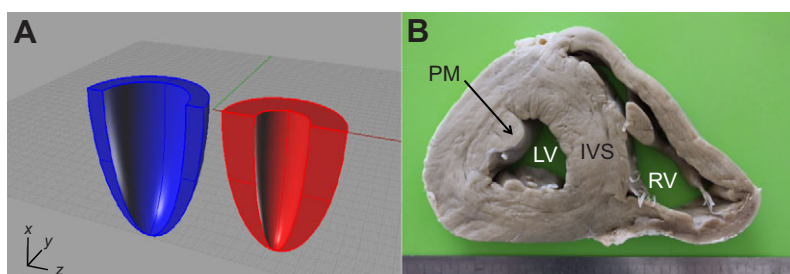


**Fig. 1. Organisation of the giraffe cardiac mass.**

(A) Computer-generated images of two hearts with identical cardiac mass; in blue is a heart with the typical mammalian organisation of cardiac tissue and in red is a heart with organisation similar to that of the giraffe. Note how the giraffe heart has both a thicker ventricular wall and a smaller cavity. (B) A short-axis view through the giraffe heart at the level of the papillary muscles. RV, right ventricle; IVS, intraventricular septum; LV, left ventricle; PM, papillary muscle.

shunts. During all rebreathing procedures, the arterial oxygen saturation exceeded 97% or above, indicating no or minimal pulmonary shunting.

### Haemodynamic parameters

A tip transducer catheter (5 French Micro-Tip SPC 350, range –50 to 400 mmHg; Millar Instruments, Houston, TX, USA) was advanced through the carotid artery into the ascending aorta for continuous recording of mean  $P_a$  using a Biopack Systems data acquisition software (AcqKnowledge 3.7.2) at 100 Hz. The second catheter was advanced into the left ventricle for measurements of left ventricular pressure ( $P_{LV}$ ).

### Echocardiography

A conventional transthoracic echocardiography probe (6T-RS TEE transducer, GE Healthcare, UK) covered with a plastic sheath was inserted into the left jugular vein through the cut-down in the neck and secured with a purse-string suture. A portable echocardiography apparatus was used for data acquisition and storage (Vivid Q, GE Healthcare, UK). For long-axis imaging, including the aortic root and valve, the mitral valve, the septum and the lateral wall of the left ventricle (similar to a five-chamber view in humans), the probe was advanced towards the right atrium just above the tricuspid valve. We measured diastolic and systolic long-axis lengths, defined as the distance from the hinge point of the anterior mitral valve leaflet to the ventricular apex. In some animals, this length exceeded the depth range of the probe, so the apex could not be defined. In these instances, the position of the apex was defined as the intersection of extrapolated lines from the septal and lateral wall endocardium. Subsequently, a partial left thoracotomy exposed the rib cage and through appropriate intercostal spaces, equatorial short and long axis video recordings were made with a conventional transthoracic echocardiographic probe (3S TTE transducer, GE Healthcare, UK). We measured the diastolic and systolic short-axis endocardial and epicardial diameters from the septum to the lateral wall, defining the right ventricular endocardial border as the septal ‘epicardium’. Diastolic and systolic wall thicknesses were measured in the septum and in the free wall. All giraffes were killed with intravenous pentobarbital (20%, KVL Pharmacy) and weighed. The heart was excised and weighed.

### Calculated haemodynamic parameters

Long-axis and short-axis shortening, and wall thickening were calculated as the absolute difference between the diastolic and systolic values divided by the diastolic value of the parameter. For calculation of chamber volumes, the left ventricle was assumed to have the shape of a prolate hemi-ellipsoid with volume:

$$V = \frac{2}{3} \pi \left( \frac{D}{2} \right)^2 L, \quad (2)$$

where  $D$  is the short axis or the diameter ( $D/2$  thus equals the internal radius of the left ventricle) and  $L$  is the long axis. Accordingly, end diastolic volume ( $V_{ED}$ ), end systolic volume ( $V_{ES}$ ), stroke volume ( $V_S$ ) and ejection fraction were calculated using the diastolic and systolic long-axis and endocardial short-axis measurements described above. Cardiac output ( $Q$ ), in absolute values and expressed relative to  $M_b$ , was calculated using the mean heart rate over the time span of the echocardiographic measurements. Taking the ellipsoid shape of the left ventricle into account, the systolic circumferential and meridional wall stresses

(CWS and MWS, respectively) were calculated in kPa as:

$$\text{CWS} = 133.322 \frac{\text{kPa}}{\text{mmHg}} \times \frac{P_{a_{\text{sys}}} \times (D/2)}{T_{\text{wall}}} \times \left( 1 - \frac{T_{\text{wall}}}{D} - \frac{(D/2)^2}{L^2} \right), \quad (3)$$

$$\text{MWS} = 133.322 \frac{\text{kPa}}{\text{mmHg}} \times \frac{P_{a_{\text{sys}}} \times (D/2)}{2 \times T_{\text{wall}} [1 + (T_{\text{wall}}/D)]}, \quad (4)$$

where  $P_{a_{\text{sys}}}$  is the mean systolic arterial pressure (mmHg) over the time span of the echocardiographic measurements,  $D$  is the systolic endocardial short-axis diameter,  $L$  is the long-axis diameter of the ventricle and  $T_{\text{wall}}$  is the systolic wall thickness (Grossman et al., 1975; Mirsky, 1969).

### Net external work by the left ventricle

Simultaneous measurements of left ventricular pressures and pulmonary flow by the inert gas rebreathing technique were performed on six animals, and allowed for net external work of the heart ( $W$ ) to be calculated as:

$$W = \Delta P_{LV} \times Q, \quad (5)$$

where  $\Delta P_{LV}$  is the change in left ventricular pressure (approximated as the systolic minus the diastolic pressure).

### Systemic vascular resistance

Systemic vascular resistance (SVR) was calculated as:

$$\text{SVR} = \frac{P_a - P_{RA}}{Q}, \quad (6)$$

where  $P_a$  is the mean arterial blood pressure,  $P_{RA}$  the right atrial pressure and  $Q$  is cardiac output.

### Diffusion tensor imaging

To visualise the three-dimensional architecture of the left ventricular myocardium in terms of cardiomyocyte pathways we performed diffusion tensor imaging (DTI) with MRI on one giraffe heart with a Philips 1.5 T Achieva system. The heart was placed in the magnet oriented with the long axis parallel to the axis of the main magnetic field, and a surface receiver coil was used for data reception. A diffusion tensor imaging sequence was applied using 32 different diffusion-weighted directions. The principal direction of the diffusion tensor was calculated in each voxel. A number of voxels of interest were selected from this three-dimensional matrix and based upon the characteristics of the primary eigenvectors; the algorithm then calculated any possible ‘track’, or pathway, which passes through the chosen voxels of interest (Smerup et al., 2009).

### Statistical analysis

Measurements were analysed with paired or unpaired  $t$ -test as appropriate. A statistical significance level of  $P < 0.05$  was used and data are expressed as means  $\pm$  s.e.m.

## RESULTS

### Ventricular dimensions and pressures *in vivo*

Echocardiography provided good visualisation of the beating giraffe heart *in vivo* (see Movie 1 and Fig. 2) and hence allowed us to determine cardiac dimensions during the entirety of the cardiac cycle. As shown by the example in Fig. 3, we obtained simultaneous measurements of aortic pressures as well as pressures within each

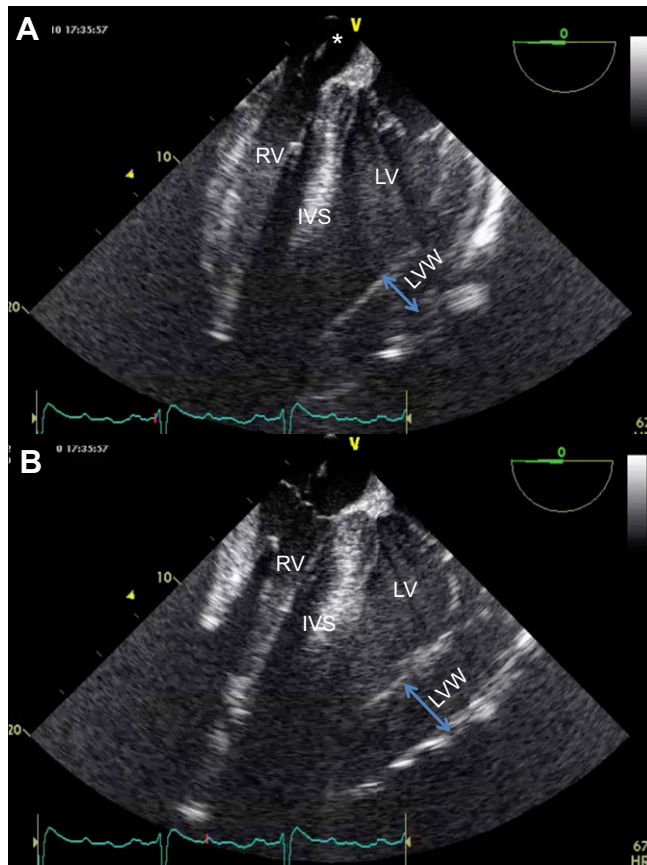


**Fig. 2.** *In vivo* intracardiac echocardiography showing long-axis view of the giraffe heart. Orientation is equivalent to four-chamber view of human heart. The probe is located in the right atrium (\*). Shown are images from the same heart cycle in one giraffe in end diastole (A) and end systole (B). Red marker on ECG trace shows temporal relation to the cardiac electrical activity. RV, Right ventricle; IVS, intraventricular septum; LV, left ventricle; LVW, left ventricular wall.

ventricle. During the echocardiography,  $P_a$  was  $224 \pm 7$  mmHg, and the systolic pressures within the left and right ventricle were  $234 \pm 7$  and  $45 \pm 3$  mmHg, respectively, with a heart rate of  $56 \pm 5$  beats  $\text{min}^{-1}$ .

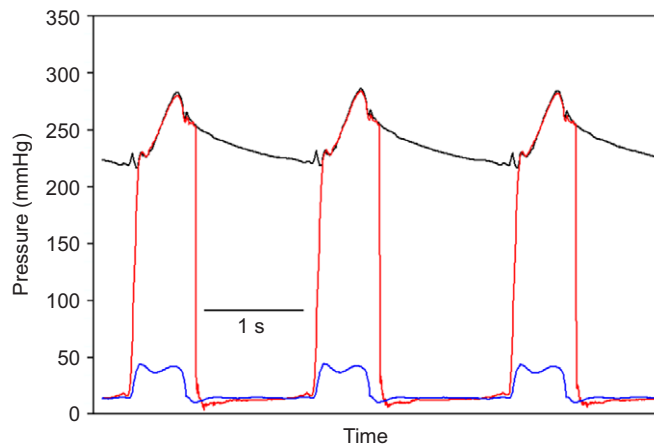


**Fig. 3.** Recording of arterial and left and the right ventricle pressure in an anaesthetised giraffe. Black,  $P_a$ ; red,  $P_{LV}$ ; blue,  $P_{RV}$ .

**Table 1.** Mean diastolic and systolic dimensions of the giraffe heart

	Diastole	Systole	Change at systole (%)
Long axis (cm)	$18.2 \pm 0.3$	$15.5 \pm 0.3$	$-14.9 \pm 0.3$
Endocardial short axis (cm)	$7.3 \pm 0.5$	$5.2 \pm 0.4$	$-28.3 \pm 3.0$
Epicardial short axis (cm)	$12.3 \pm 0.4$	$11.8 \pm 0.3$	$-3.7 \pm 2.4$
Septum (cm)	$2.9 \pm 0.1$	$3.55 \pm 0.06$	$+23.0 \pm 1.3$
Free wall (cm)	$2.15 \pm 0.04$	$3.08 \pm 0.08$	$+43.2 \pm 3.5$
Mean wall thickness to short axis ratio	$0.35 \pm 0.03$	$0.64 \pm 0.07$	–

The diastolic and systolic long-axis lengths were  $18.2 \pm 0.3$  and  $15.5 \pm 0.3$  cm, respectively ( $P < 0.001$ ), resulting in long-axis fractional shortening of  $14.9 \pm 0.3\%$ . The corresponding endocardial short-axis values were  $7.3 \pm 0.5$ ,  $5.2 \pm 0.4$  cm ( $P < 0.002$ ) and  $28.3 \pm 3.0\%$ ; epicardial values were  $12.3 \pm 0.4$  cm,  $11.8 \pm 0.3$  (NS) and  $3.7 \pm 2.4\%$ , respectively. Diastolic and systolic septal wall thicknesses were  $2.9 \pm 0.1$  and  $3.6 \pm 0.1$  cm, respectively ( $P < 0.001$ ), and thickening was  $23.0 \pm 1.3\%$ . The corresponding free wall values were  $2.2 \pm 0.1$  and  $3.1 \pm 0.1$  cm ( $P < 0.001$ ), and thickening was  $43.2 \pm 3.5\%$ . The septum was significantly thicker than the free wall in both diastole ( $P < 0.001$ ) and systole ( $P < 0.001$ ), whereas thickening in the free wall was twice that of the septum ( $P < 0.001$ ). The diastolic mean wall thickness to short-axis ratio was  $0.35 \pm 0.03$  and the corresponding systolic value was  $0.64 \pm 0.07$ . Mean diastolic dimensions, systolic dimensions and changes in dimension during systole are given in Table 1.

#### Determination of cardiac output with echocardiography and gas rebreathing

Average heart rate was  $56 \pm 5$  beats  $\text{min}^{-1}$ . Calculated  $V_{ED}$  was  $521 \pm 61$  ml or  $1.05 \pm 0.61$  ml  $\text{kg}^{-1}$  and  $ESV$  was  $228 \pm 32$  ml or  $0.46 \pm 0.83$  ml  $\text{kg}^{-1}$ , yielding an average  $V_S$  of  $293 \pm 42$  ml or  $0.59 \pm 0.42$  ml  $\text{kg}^{-1}$ , and an ejection fraction of  $55.8 \pm 3.6\%$ . Thus the echocardiographically derived cardiac output ( $Q_E$ ) was  $16.1 \pm 2.5$  l  $\text{min}^{-1}$  or  $33 \pm 12$  ml  $\text{kg}^{-1}$   $\text{min}^{-1}$ . In the 9 animals studied by the gas rebreathing procedure, the measured cardiac output ( $Q_G$ ) values ranged from  $12.0$  to  $18.7$  l  $\text{min}^{-1}$ , providing a mean of  $33 \pm 2$  ml  $\text{kg}^{-1}$   $\text{min}^{-1}$ . During inert gas rebreathing heart rate was  $58 \pm 5$  beats  $\text{min}^{-1}$ , and the calculated  $V_S$  was therefore  $278 \pm 42$  ml. An overview of calculated variables from echocardiographic data is presented in Table 2.

#### Systemic vascular resistance

In the six giraffes where we obtained simultaneous recordings of mean  $P_a$ ,  $P_{RA}$  and  $Q$  ( $234 \pm 12$  mmHg,  $5 \pm 2$  mmHg and  $15 \pm 1$  l  $\text{min}^{-1}$ , respectively), we calculated  $SVR$  to be  $16 \pm 1$  mmHg  $\text{l}^{-1}$   $\text{min}^{-1}$ .

**Table 2.** Mean calculated parameters of heart function in the giraffe

	Absolute value	Corrected value per kg
End diastolic volume, $V_{ED}$ (ml)	$521 \pm 61$	$1.05 \pm 0.61$
End systolic volume, $V_{ES}$ (ml)	$228 \pm 32$	$0.46 \pm 0.35$
Stroke volume, $V_S$ (ml)	$293 \pm 42$	$0.59 \pm 0.42$
Ejection fraction (%)	$55.8 \pm 3.6$	–
Cardiac output, $Q$ (ml $\text{min}^{-1}$ )	$16,082 \pm 2544$	$33.2 \pm 4.40$
Circumferential wall stress (kPa)	$7.83 \pm 1.76$	–
Meridional wall stress (kPa)	$7.83 \pm 0.86$	–

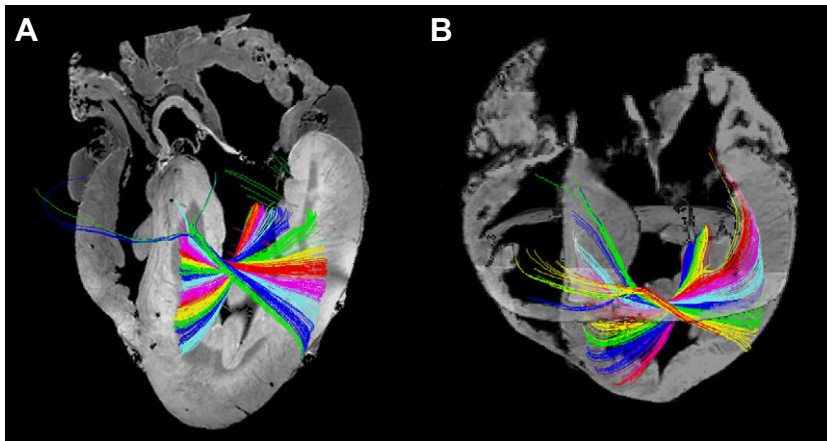


**Fig. 4. Diffusion tensor imaging of the left ventricles of a giraffe and a pig.** (A) Giraffe; (B) pig. Essentially, the DTI technique allows for visualisation of the orientation of the cardiomyocytes. There does not appear to be any significant difference in myocardial architecture of the giraffe compared with other mammals. Tracks are arbitrarily coloured to allow for easier differentiation of the orientation of the diffusion direction relative to the myocardium. The colours are therefore merely a visual aid and do not represent any anatomical or physiological properties. Images are not to scale. Likewise, please note that the images only document the principally similar myocardial architecture in pig and giraffe and that sizes are not to scale.

### Wall stresses and net external work performed by the left ventricle

Circumferential and meridional wall stresses were  $7.83 \pm 4.66$  kPa and  $7.83 \pm 2.28$  kPa, respectively. Left ventricular work averaged  $7.2 \pm 1.1$  W based on a  $\Delta P$  of  $229 \pm 14$  mmHg and a  $Q$  of  $15.0$  l  $\text{min}^{-1}$ . Heart mass was  $2.68 \pm 0.6$  kg corresponding to  $0.53 \pm 0.05\%$  of  $M_b$ . Normalised to  $M_b$ , the net external work of the heart was  $0.29$  W  $\text{kg}^{-1}$ .

### Corresponding human values

Typical corresponding values for a healthy 80 kg human with a heart rate of  $70$  beats  $\text{min}^{-1}$  would be a  $V_{ED}$  of  $150$  ml or  $1.88$  ml  $\text{kg}^{-1}$ , a  $V_{ES}$  of  $70$  ml or  $0.88$  ml  $\text{kg}^{-1}$ , a  $V_S$  of  $80$  ml or  $1$  ml  $\text{kg}^{-1}$ , an ejection fraction of  $53.3\%$  and  $Q$  of  $5.6$  l  $\text{min}^{-1}$  or  $70$  ml  $\text{kg}^{-1}$   $\text{min}^{-1}$ . With a mean  $P_a$  of  $80$  mmHg, a systolic pressure of  $110$  mmHg and a  $P_{RA}$  of  $5$  mmHg, the SVR would be  $13.4$  mmHg  $\text{l}^{-1}$   $\text{min}^{-1}$  and circumferential and meridional wall stresses would be  $8.91$  kPa and  $2.90$  kPa, respectively.

### Diffusion tensor imaging

An example of the tracking of the ventricular myocytes in the giraffe heart is shown in Fig. 4, where we use a similar visualisation of the cardiomyocytes of the pig heart for comparison. The principal myocardial architecture of the giraffe left ventricle, i.e. the so-called helical angle distribution (the inclination of the cardiomyocyte tracks relative to the equatorial plane of the left ventricle), as well as the pattern of myocardial pathways, did not reveal any obvious differences compared with other mammals (Scollan et al., 1998; Smerup et al., 2009).

### DISCUSSION

Our *in vivo* echocardiography revealed that the giraffe heart is characterised by a small left ventricular cavity and hence a small ventricular radius as well as a comparatively large left ventricular myocardial wall thickness, which has only been inferred previously from post mortem observations (Mitchell and Skinner, 2009; Østergaard et al., 2013). Since we also confirmed the conspicuously high mean  $P_a$  and the associated high intraventricular pressures in the giraffe, our findings support the hypothesis that the combination of thick left ventricular wall and a low radius of the left ventricular cavity allow for a normal mammalian myocardial wall stress in the giraffe heart. In fact, the calculated wall stress of the left ventricle in the giraffes is virtually identical to that reported for other mammals (Seymour and Blaylock, 2000). The low  $V_S$  is corroborated by the independent measures of low CO using the inert gas-rebreathing

technique, and it is clear therefore that the normalisation of ventricular wall stress by the low radius ventricle constrains oxygen delivery by the cardiovascular system.

Based on our own preliminary tracking of the cardiomyocytes in the giraffe left ventricle, there does not appear to be any significant principal differences in the myocardial architecture between the giraffe and other mammals (Nielsen et al., 2009; Smerup et al., 2009). Therefore, there is no indication that giraffes have evolved cardiomyocytes generating excessive force or other peculiar adaptations; instead, the ability to develop a sufficiently high pressure for cerebral perfusion in the standing position can merely be ascribed to the thick myocardial wall and the small radius. We found that the giraffe meridional and circumferential wall stresses were identical. This is interesting because the former value normally exceeds the latter, and this might indicate that giraffe left ventricles have slightly altered myocardial architecture that possibly serves to redistribute myocardial stresses differently during cardiac contraction in comparison to the myocardium of other species, which exhibit a lower ventricular wall thickness to cavity diameter ratio ( $T_{\text{wall}}/D$ ).

Indeed, the altered  $T_{\text{wall}}/D$  ratio in the adult giraffe seems to be an example of a beneficial physiological adaptation to a naturally high

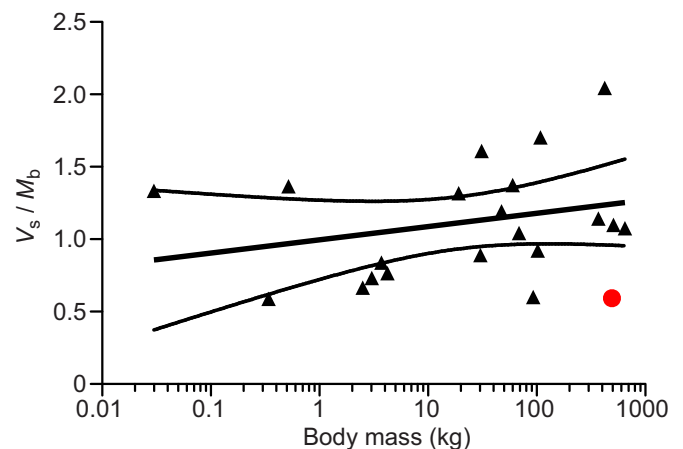


**Fig. 5. Corrected stroke volume as a function of total body mass in various extant mammal species.** Data are from Seymour and Blaylock, 2000. The solid line indicates the semi-log regression line calculated on the basis of these values, stippled lines indicate the calculated 95% confidence interval. Shown in red is the corresponding value for giraffes reported in the present study.

mean  $P_a$ , caused by a high SVR, which is in itself an adaptation to the perfusion requirements of the brain. Thus, although the thick ventricular wall resembles the pathophysiological changes during acquired ventricular hypertrophy in response to aortic stenosis or hypertension in humans (Grossman et al., 1975; Hood et al., 1968; Sandler and Dodge, 1963), there is no indication of the secondary myocardial fibrosis in giraffes that inevitably accompanies the acquired left ventricular hypertrophy observed in human disease. It is also noteworthy that newborn giraffes have a myocardial wall thickness relative to ventricular diameter that is similar to other mammals, such that the ventricular wall thickening seems to arise as mean  $P_a$  increases with neck length (Mitchell and Skinner, 2009). Because the ventricular remodelling develops in response to increased afterload as the giraffe grows taller and because total myocardial volume of adult giraffes resembles that of similar-sized mammals, we suggest that the term ‘concentric eutrophy’ is used for the normal physiological state of the adult giraffe myocardium. The low cardiac output of giraffes alleviates the influence of the high mean  $P_a$  on the workload of the heart. Our estimation of cardiac workload in the giraffe ( $0.29 \text{ W kg}^{-1}$  heart) is very similar, for example, to the workload of the healthy human heart ( $0.36 \text{ W kg}^{-1}$  heart).

Our echocardiography also revealed a normal mammalian ejection fraction, and hence low ventricular volumes, i.e.  $V_{ED}$ ,  $V_{ES}$  and  $V_S$  were almost half of those in similar-sized mammals. This is illustrated in Fig. 5 depicting reported  $V_S$  in mammals (Seymour and Blaylock, 2000) as a function of body mass. The calculation of volumes based on echocardiography relies upon the assumption that the left ventricle is shaped like a prolate hemi-ellipsoid, but the low volumes were also confirmed independently by the measurements using the inert gas rebreathing technique. Determination of cardiac output by inert gas rebreathing relies on gas clearance in the lungs over multiple heartbeats and is therefore methodologically distinct from echocardiographic methods relying on beat-to-beat changes in ventricular volume. Thus, our study provides strong evidence for a considerably lower cardiac output in giraffes than in other similar-sized mammals. In the literature, we are aware of only two earlier studies of cardiac output, providing data from a total of eight measurements in five giraffe specimens, but several of the values were not corrected for body mass. Goetz et al. (1960) used both indicator-dye dilution and the direct Fick methods in one ill and three healthy giraffes (values are reported for three of the animals). The authors described difficulties with the dye-dilution technique, but obtained cardiac output measurements of  $48$  and  $78 \text{ ml kg}^{-1} \text{ min}^{-1}$  using direct Fick in the two individuals where body mass was estimated ( $500$  and  $455 \text{ kg}$ , respectively). In the only other study, Linton et al. (1999) were surprised to measure a cardiac output of only  $20 \text{ l min}^{-1}$  (equivalent to  $25 \text{ ml kg}^{-1} \text{ min}^{-1}$ ) in an  $800 \text{ kg}$  giraffe using a lithium dilution technique. This value fits remarkably well with our measurements.

Our work also confirms that the systemic vascular resistance (SVR) of giraffes is considerably higher than that of other similar-sized mammals. Given the low cardiac output, the high SVR is required to support the high mean  $P_a$  necessary to perfuse the brain, but our study does not provide insight into the specific mechanisms underlying the high resistance. Previous studies have reported thick blood vessel walls with a high wall-to-lumen ratio (e.g. Hargens et al., 1988; Keen and Goetz, 1957; Kimani et al., 1991; Østergaard et al., 2011; Petersen et al., 2013), but there is clearly a need to study the resistance of vessels throughout the vasculature in more detail.

The myocardial remodelling clearly seems adaptive to the high mean  $P_a$  required for cerebral perfusion, but the resultant decrease in

$V_S$  obviously imposes a potential limitation to systemic oxygen delivery. The rate of oxygen consumption of anaesthetised giraffes resembles that of similar-sized mammals (Langman et al., 1982), and the low  $V_S$  is in any event unlikely to constrain resting metabolism because an increased arterial–venous oxygen extraction could suffice. In free-moving awake giraffes, van Citters et al. (1969) reported that heart rate increased from around  $40 \text{ beats min}^{-1}$  in undisturbed quietly standing giraffes to maximum values of  $175 \text{ beats min}^{-1}$  during galloping when actively chased on the savannah. It remains to be determined whether this more than fourfold rise in heart rate is accompanied by altered  $V_S$ , but the thick ventricular wall probably lowers ventricular compliance and it could be speculated to constrain the ability for the ventricle to alter  $V_S$ . Thus, the low  $V_S$  probably persists during exercise and constrains aerobic performance, and hence limits the maximal aerobic running speed. However, the long legs of giraffes appear to reduce energy expenditure required for transport (Pontzer, 2007). Thus, as  $V_S$  became increasingly constrained by concentric eutrophy of the ventricle in response to the progressive evolution of a longer neck (i.e. increasing the vertical distance between the heart and head and thus requiring higher mean  $P_a$ ), the requirements on oxygen delivery during locomotion were probably alleviated, as the legs also got longer. Clearly, this speculation needs to be supported by measurements of field metabolic rate (e.g. using double-labelled water) and the associated cardiovascular responses to estimate cost of locomotion in free-ranging giraffes.

It can be calculated that a ‘perfect left ventricle’, i.e. a pumping chamber that achieves the high mean  $P_a$  of giraffes and thus retains the beneficial ratio of radius versus wall thickness reported here while still being able to generate a cardiac output per body mass unit comparable to other mammalian species would have an  $V_{ED}$  of  $1060 \text{ ml}$  and a  $V_S$  of  $583 \text{ ml}$ , which is approximately twice the measured values. The cavity radius would be  $4.7 \text{ cm}$  and the myocardial wall thickness  $3.3 \text{ cm}$ . As it is not easy to calculate the total mass of this hypothetical pump, it can only be speculated that the energy cost of such an organ would likewise exceed the average mammalian value by a factor of two or three.

The main limitation to the present study is the use of linear dimensions measured with echocardiography to determine left ventricular volumes by assuming the fairly simple prolate hemi-ellipsoidal geometry. This method has obviously not been validated because our study is the first to report the use of echocardiography on the giraffe heart and no gold standard for measurements in this species exists. By virtue of the same argument, we did not use Simpson’s method (Folland et al., 1979) or other indirect methods for volume assessment.

In conclusion, our study supports the notion that relative myocardial mass is fairly invariant amongst mammals. The phenotypical adaptations to the high arterial pressures in giraffes have been achieved by evolving a low volume, low flow pump that is suitable to maintain cerebral perfusion, but imposes limitations on cardiac chamber size and stroke volume and possibly on maximum sustainable rate of oxygen consumption.

#### Acknowledgements

We thank all members of the DaGir expedition and the staff at Wildlife Assignment International, South Africa, for assistance with numerous details in relation to handling of giraffes. Peter Agger Nielsen graciously supplied the DTMRI images of the giraffe heart. We also thank Frederik, Christian and Lisbeth Secher for practical assistance.

#### Competing interests

The authors declare no competing or financial interests.

**Author contributions**

All authors contributed to the idea, conception, experimental design, experiments and analysis of the data. M.S., M.D. and T.W. collated the data and wrote the manuscript. All authors approved and contributed to the final version.

**Funding**

The study was supported by the Lundbeck Foundation, Carlsbergfondet, The Danish Heart Association, the Aase and Ejnar Danielsen Foundation, The Danish Research Council, The Danish Cardiovascular Research Academy, Nyforeningens Forskningsfond, Fonden til Lægevidenskabens Fremme, The Faculty of Health Science and the Faculty of Natural Sciences at Aarhus University, and the Aarhus University Research Foundation.

**Supplementary information**

Supplementary information available online at  
<http://jeb.biologists.org/lookup/suppl/doi:10.1242/jeb.132753/-DC1>

**References**

- Brøndum, E., Hasenkam, J. M., Secher, N. H., Bertelsen, M. F., Grøndahl, C., Petersen, K. K., Buhl, R., Aalkjær, C., Baandrup, U., Nygaard, H. et al.** (2009). Jugular venous pooling during lowering of the head affects blood pressure of the anesthetized giraffe. *Am. J. Physiol.* **297**, R1058–R1065.
- Clemensen, P., Christensen, P., Norsk, P. and Grønlund, J.** (1994). A modified photo- and magnetoacoustic multigas analyzer applied in gas exchange measurements. *J. Appl. Physiol.* **76**, 2832–2839.
- Covert, R. F., Schreiber, M. D., Leff, A. R., White, S. R., Munoz, N. M. and Torgerson, L. J.** (1992). Oxygen metabolism and catecholamine secretion during chloralose anesthesia in lambs. *J. Dev. Physiol.* **17**, 125–132.
- Crisp, E.** (1864a). Contributions to the anatomy of the giraffe, with an account of the length of the alimentary canal of many other ruminants. *Proc. Zool. Soc.*, 63–68.
- Crisp, E.** (1864b). Further contributions to the anatomy of the giraffe and the nyghau. *Proc. Zool. Soc.*, 269–271.
- Folland, E. D., Parisi, A. F., Moynihan, P. F., Jones, D. R., Feldman, C. L. and Tow, D. E.** (1979). Assessment of left ventricular ejection fraction and volumes by real-time, two-dimensional echocardiography. A comparison of cineangiographic and radionuclide techniques. *Circulation* **60**, 760–766.
- Gabrielsen, A., Videbæk, R., Schou, M., Damgaard, M., Kastrop, J. and Norsk, P.** (2002). Non-invasive measurement of cardiac output in heart failure patients using a new foreign gas rebreathing technique. *Clin. Sci.* **102**, 247–252.
- Goetz, R. H.** (1955). Preliminary observations on the circulation in the giraffe. *Trans. Am. Coll. Cardiol.* **5**, 239–248.
- Goetz, R. H.** (1956). The giraffe. *Lancet* **271**, 351.
- Goetz, R. H. and Budtz-Olsen, O.** (1955). Scientific safari - the circulation of the giraffe. *S. A. Med. J.* **29**, 773–776.
- Goetz, R. H. and Keen, E. N.** (1957). Some aspects of the cardiovascular system in the giraffe. *Angiology* **8**, 542–564.
- Goetz, R. H., Warren, J. V., Gauer, O. H., Patterson, J. L., Doyle, J. T., Keen, E. N. and McGregor, M.** (1960). Circulation of the giraffe. *Circ. Res.* **8**, 1049–1058.
- Grossman, W., Jones, D. and McLaurin, L. P.** (1975). Wall stress and patterns of hypertrophy in the human left ventricle. *J. Clin. Invest.* **56**, 56–64.
- Hargens, A. R., Gershuni, D. H., Danzig, L. A., Millard, R. W. and Petterson, K.** (1988). Tissue adaptations to gravitational stress - newborn versus adult giraffes. *Physiologist* **31**, 110–113.
- Hood, W. P., Jr., Rackley, C. E. and Rolett, E. L.** (1968). Wall stress in the normal and hypertrophied human left ventricle. *Am. J. Cardiol.* **22**, 550–558.
- Keen, E. N. and Goetz, R. H.** (1957). Cardiovascular anatomy of a foetal giraffe. *Acta Anat.* **31**, 562–571.
- Kimani, J. K., Mbuva, R. N. and Kinyamu, R. M.** (1991). Sympathetic innervation of the hindlimb arterial system in the giraffe (*Giraffa camelopardalis*). *Anat. Rec.* **229**, 103–108.
- Langman, V. A., Bamford, O. S. and Maloiy, G. M. O.** (1982). Respiration and metabolism in the giraffe. *Respir. Physiol.* **50**, 141–152.
- Linton, R. A. F., Taylor, P. M., Linton, N. W. F., Flach, E. J., O'Brien, T. K. and Band, D. M.** (1999). Cardiac output measurement in an anaesthetised giraffe. *Vet. Rec.* **145**, 498–499.
- Mirsky, I.** (1969). Left ventricular stresses in the intact human heart. *Biophys. J.* **9**, 189–208.
- Mitchell, G. and Skinner, J. D.** (2009). An allometric analysis of the giraffe cardiovascular system. *Comp. Biochem. Physiol. A Mol. Integr. Physiol.* **154**, 523–529.
- Mitchell, G., Maloney, S. K., Mitchell, D. and Keegan, D. J.** (2006). The origin of mean arterial and jugular venous blood pressures in giraffes. *J. Exp. Biol.* **209**, 2515–2524.
- Nielsen, E., Smerup, M., Agger, P., Frandsen, J., Ringgaard, S., Pedersen, M., Vestergaard, P., Nyengaard, J. R., Andersen, J. B., Lunkenheimer, P. P. et al.** (2009). Normal right ventricular three-dimensional architecture, as assessed with diffusion tensor magnetic resonance imaging, is preserved during experimentally induced right ventricular hypertrophy. *Anat. Rec.* **292**, 640–651.
- Østergaard, K. H., Bertelsen, M. F., Brøndum, E. T., Aalkjær, C., Hasenkam, J. M., Smerup, M., Wang, T., Nyengaard, J. R. and Baandrup, U.** (2011). Pressure profile and morphology of the arteries along the giraffe limb. *J. Comp. Physiol. B* **181**, 691–698.
- Østergaard, K. H., Baandrup, U. T., Wang, T., Bertelsen, M. F., Andersen, J. B., Smerup, M. and Nyengaard, J. R.** (2013). Left ventricular morphology of the giraffe heart examined by stereological methods. *Anat. Rec.* **296**, 611–621.
- Perez, W., Lima, M., Pedrana, G. and Cirillo, F.** (2008). Heart anatomy of *Giraffa camelopardalis rothschildi*: a case report. *Vet. Med.* **53**, 165–168.
- Petersen, K. K., Hørlyck, A., Østergaard, K. H., Andresen, J., Brøgger, T., Skovgaard, N., Telinius, N., Laher, I., Bertelsen, M. F., Grøndahl, C. et al.** (2013). Protection against high intravascular pressure in giraffe legs. *Am. J. Physiol. Cell Physiol.* **305**, R1021–R1030.
- Pontzer, H.** (2007). Effective limb length and the scaling of locomotor cost in terrestrial animals. *J. Exp. Biol.* **210**, 1752–1761.
- Rosenberg, M.** (1999). *Non-Violent Communication: A Language of Compassion*. Encinitas, CA: Puddledancer Press.
- Sandler, H. and Dodge, H. T.** (1963). Left ventricular tension and stress in man. *Circ. Res.* **13**, 91–104.
- Scollan, D. F., Holmes, A., Winslow, R. and Forder, J.** (1998). Histological validation of myocardial microstructure obtained from diffusion tensor magnetic resonance imaging. *Am. J. Physiol.* **275**, H2308–H2318.
- Seymour, R. S. and Blaylock, A. J.** (2000). The principles of Laplace and scaling of ventricular wall stress and blood pressure in mammals and birds. *Physiol. Biochem. Zool.* **73**, 389–405.
- Smerup, M., Nielsen, E., Agger, P., Frandsen, J., Vestergaard-Poulsen, P., Andersen, J., Nyengaard, J., Pedersen, M., Ringgaard, S., Hjortdal, V. et al.** (2009). The three-dimensional arrangement of the myocytes aggregated together within the mammalian ventricular myocardium. *Anat. Rec.* **292**, 1–11.
- Van Citters, R. L., Kemper, W. S. and Franklin, D. L.** (1966). Blood pressure responses of wild giraffes studied by radio telemetry. *Science* **152**, 384–386.
- Van Citters, R. L., Kemper, W. S. and Franklin, D. L.** (1968). Blood flow and pressure in the giraffe carotid artery. *Comp. Biochem. Physiol.* **24**, 1035–1042.
- Van Citters, R. L., Franklin, D. L., Vatner, S. F., Patrick, T. and Warren, J. V.** (1969). Cerebral hemodynamics in the giraffe. *Trans. Assoc. Am. Physicians* **82**, 293–304, 1969.